Analysis of Mixed-mode Crack Propagation by the Movable Cellular Automata Method

Young Suck Chai[1,#], Choon-Yeol Lee[1] and Mikhail Pak[1]

1 School of Mechanical Engineering, Yeungnam University 214-1 Dae-Dong, Gyongsan, Kyungbuk, South Korea, 712-749
Corresponding Author / E-mail: yschai@yu.ac.kr, TEL: +82-53-810-2464, FAX: +82-53-810-4627

KEYWORDS: Mixed-mode crack, Movable Cellular Automata, Crack initiation criteria, Stress intensity factor, Energy release rate, Bifurcation angle

The propagation of a mixed-mode crack in soda-lime silica glass is modeled by movable cellular automata (MCA). In this model, a special fracture criterion is used to describe the process of crack initiation and propagation. The results obtained using the MCA criterion are compared to those obtained from other crack initiation criteria. The crack resistance curves and bifurcation angles are determined for various loading angles. The MCA results are in close agreement with results obtained using the maximum circumferential tensile stress criterion.

Manuscript received: February 20, 2008 / Accepted: July 27, 2008

NOMENCLATURE

a = crack length
$d^{i(j)}$ = automata size
E' = modulus of elasticity
G = energy release rate
h^{ij} = overlapping parameter in the i-j pair
K^{ij} = effective adhesion coefficient
K_I, K_{II} = stress intensity factors corresponding to pure mode I and mode II loading, respectively.
K_{IC} = critical stress intensity factor corresponding to pure mode I
l = infinitesimal "kink"
r^{ij} = distance between the centers of the neighboring elements in the i-j pair
S = strain energy density factor
V = unit volume
W = strain energy density
δ^{ij} = generalized switching parameter in the i-j pair
μ = shear modulus
ν = Poisson's ratio
θ_0 = bifurcation angle
θ^{ij} = angle of relative rotation in the i-j pair
σ^{ij}_{int} = stress intensity in the i-j pair
σ^{ij}_x, σ^{ij}_y = normal i-j pair stress in the x and y directions, respectively
σ_s = ultimate strength
τ^{ij} = shear i-j pair stress
ψ = loafing angle

1. Introduction

Cellular automata were originally conceived by Ulam and von Neumann in the 1940s to provide a formal framework for investigating the behavior of complex extended systems.[1] A cellular automata consists of a regular grid of cells, each of which can be in any one of a finite number of k-possible states, updated synchronously in discrete time steps according to a local interaction rule that is the same for all cells. The state of a cell is determined by the previous states of a surrounding neighborhood of cells.[2] Over the years, cellular automata have been applied to a broad range of phenomena, including communication, computation, construction, growth, reproduction, competition, and evolution.[3-5]

Psakhie[6,7] and his associates introduced the movable cellular automata (MCA) technique, which makes use of the state of a pair of automata (*i.e.*, a relationship between an interacting pair of automata) in addition to the conventional state of a single automaton. This method allows the evolution of the net concept to the neighbor concept. As a result, the automata have the ability to change their neighbors by switching the states of pairs.

Crack propagation has been studied extensively during the past several decades. Various fracture criteria have been proposed to describe the mechanism of crack growth, including criteria based on the stress intensity factor, strain energy release rate, J-integral, crack tip opening displacement (CTOD), crack tip opening angle, strain energy density, void nucleation, and so forth.[8-12] The current work presents a new type of fracture criterion that explains the crack growth process based on the MCA method.

2. MCA Background

The MCA method introduces the state of a pair of automata, in addition to the conventional state of a single automaton. This definition allows the evolution of the net concept to the neighbor concept. As a result, the automata are capable of changing their neighbors by switching the states of pairs.[7] The criterion for switching inter-automata relationships is expressed in terms of the automata overlapping parameter, defined by

$$h^{ij} = r^{ij} - r_o^{ij} \tag{1}$$

Here r^{ij} is the distance between the centers of the neighboring elements, and r_o^{ij} is defined as

$$r_o^{ij} = (d^i + d^j)/2 \tag{2}$$

where $d^{i(j)}$ is the size of the automata.

In accordance with the concept of bistable automata, there are two types of pair states (relationships): linked and unlinked. In the simplest case, linked refers to a pair of automata joined by a chemical bond, and unlinked refers to a pair of automata having no chemical bond between them. On both the meso-scale and macro-scale levels, rotation must also be considered. The rotation parameter θ^{ij} is the angle of relative rotation in the *i-j* pair. (It is also used as a switching parameter, analogous to the translational parameter h^{ij}.) In the most general case, these two parameters can be combined into one generalized parameter:

$$\delta^{ij} = F(h^{ij}, \theta^{ij}) \tag{3}$$

The linked→unlinked switch then takes place when δ^{ij} reaches the threshold value of δ^{ij}_{max}.

Hence, changes of pair states are controlled by the relative movements of the automata, and the medium formed by such pairs can be considered a bistable medium. The initial structure is formed by setting up certain relationships between each pair of neighboring elements.

In MCA, stress intensity is also used as a parameter for the linked→unlinked switch. The stress intensity for the i^{th} automaton in the *i-j* pair is calculated as follows:

$$\sigma_{\text{int}}^{ij} = \sqrt{\left(\sigma_x^{ij}\right)^2 + \left(\sigma_y^{ij}\right)^2 - \sigma_x^{ij}\sigma_y^{ij} + 3\left(\tau^{ij}\right)^2} \tag{4}$$

where σ^{ij}_x and σ^{ij}_y are the normal *i-j* pair stresses, and τ^{ij} is the shear stress.

The stress intensity for j^{th} automaton in the *i-j* pair is calculated similarly. When the i^{th} and j^{th} automata have the same material properties, the ultimate strength σ_s is used as a threshold value:

$$\text{unlinked when } \sigma_{\text{int}}^{ij} \geq K^{ij}\sigma_S^i \tag{5}$$

In general, the automata in the *i-j* pair consist of different materials with different physico-mechanical properties. In this case, the threshold value for the linked→unlinked switch depends not only on the strength of both materials, but also on the inter-automata adhesion (*i.e.*, the bond formation history). The following general criterion is therefore proposed:

$$\text{unlinked when } \begin{cases} \sigma_{\text{int}}^{ij} \geq K^{ij}\sigma_S^i \\ or \\ \sigma_{\text{int}}^{ji} \geq K^{ij}\sigma_S^j \end{cases} \tag{6}$$

Here $\sigma^{i(j)}_s$ is the strength of the $i(j)^{th}$ automata and K^{ij} is the effective adhesion coefficient. The range of values for K^{ij} is $[0, \infty)$. The specific value of K^{ij} depends a number of factors, including the history of intermaterial adhesion formation, the size of the automata, *etc.* When the automata have the same material properties, $K^{ij} = 1$.

3. Crack Initiation Criteria

3.1 Maximum Circumferential Tensile Stress Criterion

Using Irwin's concept of stress intensity factors (which characterize the strength of the singularity at a crack tip), the near crack tip ($r << a$) stresses can be written in either Cartesian coordinates or polar coordinates.[13] Erdogan and Sih[14] presented the maximum circumferential tensile stress theory as a mixed-mode fracture initiation theory. The maximum tensile stress criterion is based on a polar coordinate representation of the stress state near the tip of a crack. The maximum circumferential tensile stress theory states that crack extension starts at the tip and continues in a radial direction. Moreover, crack extension begins in the plane perpendicular to the direction of greatest tension (*i.e.*, at an angle θ_0 such that $\tau_{r\theta} = 0$ when $\sigma_{\theta max}$ reaches a critical value).

When crack extension is possible, the maximum circumferential tensile stress σ_θ can be written as

$$\sigma_\theta = \frac{K_I}{\sqrt{2\pi r}}\cos\frac{\theta_0}{2}\left(1 - \sin^2\frac{\theta_0}{2}\right) + \frac{K_{II}}{\sqrt{2\pi r}}\left(-\frac{3}{4}\sin\frac{\theta_0}{2} - \frac{3}{4}\sin\frac{3\theta_0}{2}\right) \tag{7}$$

A critical value should be obtainable by simplifying the previous equation as follows:

$$\sigma_{\theta\max}\sqrt{2\pi r} = K_{IC} = \cos\frac{\theta_0}{2}\left(K_I\cos^2\frac{\theta_0}{2} - \frac{3}{2}K_{II}\sin\theta_0\right) \tag{8}$$

The resulting equation can be normalized, and the crack initiation angle can then be obtained from

$$\frac{K_I}{K_{IC}}\cos^3\frac{\theta_o}{2} - \frac{3}{2}\frac{K_{II}}{K_{IC}}\cos\frac{\theta_o}{2}\sin\theta_o = 1 \tag{9}$$

3.2 Maximum Energy Release Rate Criterion

Erdogan and Sih[14] noted that if we utilize the Griffith energy theory as a criterion for predicting crack growth, the crack will grow in the direction of the maximum elastic energy release per unit crack extension, and the crack will start to grow when this energy reaches a critical value. A mathematical expression of $G(da,\theta)$ was discovered by Hussain, Pu, and Underwood.[15] As illustrated in Fig. 1, $K_I(\theta)$ and $K_{II}(\theta)$, the stress intensity factors of a major crack having an infinitesimal "kink" at an angle θ, can be expressed in terms of K_I and K_{II}, the stress intensity factors of the original crack.:

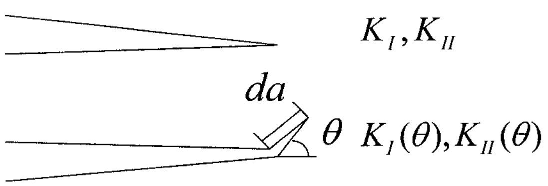

Fig. 1 Crack with an infinitesimal "kink" at angle θ

$$\begin{Bmatrix} K_I(\theta) \\ K_{II}(\theta) \end{Bmatrix} = \left(\frac{4}{3 + \cos^2\theta}\right)\left(\frac{1 - \frac{\theta}{\pi}}{1 + \frac{\theta}{\pi}}\right)^{\frac{\theta}{2\pi}} \begin{Bmatrix} K_I\cos\theta + \frac{3}{2}K_{II}\sin\theta \\ K_{II}\cos\theta - \frac{1}{2}K_I\sin\theta \end{Bmatrix} \tag{10}$$

These formulae for $K_I(\theta)$ and $K_{II}(\theta)$ can be substituted into Irwin's generalized expression for the energy release rate, which yields:

$$G(\theta) = \left(\frac{1}{E'}\right)(K_I^2(\theta) + K_{II}^2(\theta)) \tag{11}$$

$$G(\theta) = \frac{4}{E'}\left(\frac{1}{3 + \cos^2\theta}\right)^2\left(\frac{1 - \frac{\theta}{\pi}}{1 + \frac{\theta}{\pi}}\right)^{\frac{\theta}{\pi}}[(1 + 3\cos^2\theta)K_I^2 + 8\sin\theta\cos\theta K_I K_{II} + (9 - 5\cos^2\theta)K_{II}^2] \tag{12}$$

The angle of crack propagation θ_0 is obtained by maximizing $G(\theta)$:

$$\frac{\partial G(\theta)}{\partial\theta}=0 \text{ and } \frac{\partial^2 G(\theta)}{\partial^2\theta}<0 \quad (13)$$

If crack extension occurs when G reaches a critical value that is the same scalar quantity in all cases, this critical value can be determined by setting $K_{II} = 0$ and $G_C = K^2_{IC} / E$. Based on this criterion, the angle prediction equation is given by:

$$4\left(\frac{1}{3+\cos^2\theta}\right)^2\left(\frac{1-\frac{\theta_o}{\pi}}{1+\frac{\theta_o}{\pi}}\right)^{\frac{\theta_0}{\pi}}[(1+3\cos^2\theta_o)\left(\frac{K_I}{K_{IC}}\right)^2 + 8\sin\theta_o\cos\theta_o\left(\frac{K_I K_{II}}{K_{IC}^2}\right)+(9-5\cos^2\theta_o)\left(\frac{K_{II}}{K_{IC}}\right)^2]=1 \quad (14)$$

3.3 Minimum Strain Energy Density Criterion

The minimum strain energy density theory, formulated by Sih,[16] postulates that a fracture initiates from the crack tip in a direction θ_0, such that the strain energy density is minimal at a critical distance (*i.e.*, the crack propagates along a path of minimum resistance).

The strain energy density dW per unit volume dV is

$$\frac{dW}{dV}=\frac{1}{2}(\sigma_x^2+\sigma_y^2+\sigma_z^2)-\frac{\nu}{E}(\sigma_x\sigma_y+\sigma_y\sigma_z+\sigma_z\sigma_x)+\frac{1}{2\mu}(\tau_{xy}^2+\tau_{yz}^2+\tau_{zx}^2) \quad (15)$$

where μ is the shear modulus. In the two-dimensional case, the equation reduces to

$$\frac{dW}{dV}=\frac{1}{4\mu}\left[\frac{1+k}{4}(\sigma_x^2+\sigma_y^2)-2(\sigma_x\sigma_y-\tau_{xy}^2)\right] \quad (16)$$

where $k = 3 - 4\nu$ for planar strain and $k = (3 - 4\nu) / (1 + \nu)$ for planar stress, respectively. Inserting the near tip stress field into Eq. (16) yields:

$$\frac{\partial W}{\partial V}=\frac{1}{r_0\pi}(a_{11}K_I^2+2a_{12}K_IK_{II}+a_{22}K_{II}^2)=\frac{S(\theta)}{r_0} \quad (17)$$

where $$a_{11}=\frac{1}{16\mu}[(1+\cos\theta)(k-\cos\theta)] \quad (18)$$

$$a_{12}=\frac{\sin\theta}{16\mu}[2\cos\theta-(k-1)] \quad (19)$$

$$a_{22}=\frac{1}{16\mu}[(1+k)(1-\cos\theta)+(1+\cos\theta)(3\cos\theta-1)] \quad (20)$$

By the assumptions of this model, the direction of fracture initiation is toward the point of the minimal strain energy density factor S_{min} ($\partial S/\partial\theta = 0$, and $\partial^2 S/\partial^2\theta > 0$). Moreover, fracture initiation is assumed to occur when $S_{\theta min}$ reaches the maximum critical value S_C. If we set $K_{II} = 0$, then $\theta_0 = 0$ and $S_C =$ `$(S(\theta))_{min} = S(\theta = 0) = a_{11}K_{IC}$. Thus

$$S_C=\frac{(k-1)}{8\pi\mu}K_{IC}^2 \quad (21)$$

Upon minimizing the strain energy density factor, the fracture locus is given by

$$\frac{8\mu}{(k-1)}[a_{11}\left(\frac{K_I}{K_{IC}}\right)^2+2a_{12}\left(\frac{K_IK_{II}}{K_{IC}^2}\right)+a_{22}\left(\frac{K_{II}}{K_{IC}}\right)^2]=1 \quad (22)$$

4. Numerical Simulation

A compact tension-shear (CTS) specimen was used to model the process of crack propagation (Fig. 2). The material was soda-lime silica glass with the following properties: E = 68 GPa, ν = 0.19, and σ_S = 69 MPa. The analysis was done with the MCA 2D Loading Test program based on the MCA method. Plane stress conditions were used. Increasing tensile and shear stresses were applied simultaneously with various values of $\psi = tan^{-1}[(\tau_{xy})_\infty/(\sigma_y)_\infty]$. The total number of automata was about 57000. As described above, space is represented in the MCA method by discrete elements of diameter d,

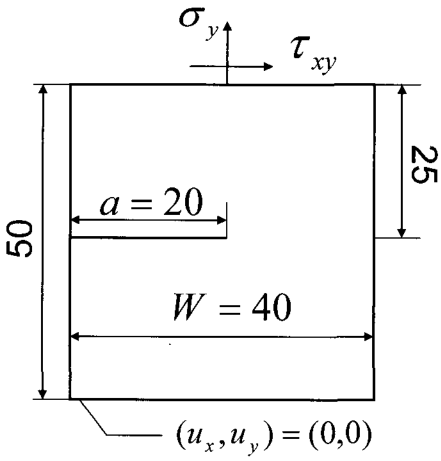

Fig. 2 CTS Specimen (dimensions in mm)

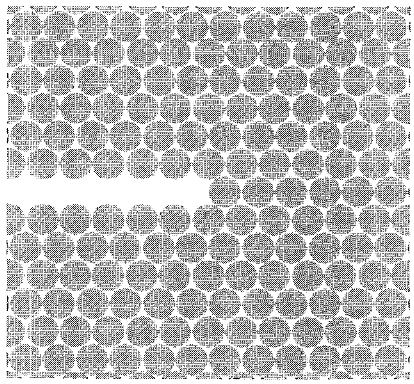

(a) automata view

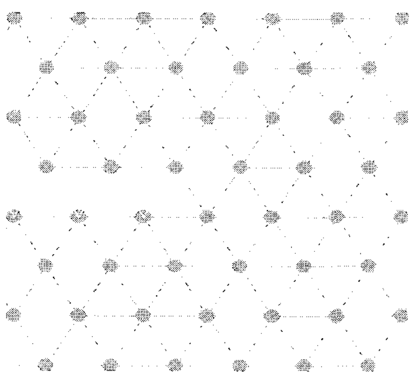

(b) link view

Fig. 3 MCA geometrical models magnified near the crack tip called automata. As shown in Fig. 3, each element is connected to its nearest neighbors (linked elements), except for the elements lying on the crack line (unlinked elements). As the normal and shear stresses are increased (with ψ held constant), the local stress around the crack tip increases until it reaches the critical value of Eq. (1), and the first link on the crack tip is broken. This was taken to be the definition of crack initiation. At this instant, the critical tensile and shear stresses obtained from the MCA analysis were used as input data for the ANSYS finite element package to calculate the stress intensity factors for mixed-mode loading. The same procedure was used to construct the resistance curve and calculate the J-integral.

5. Results and Discussion

The crack growth paths obtained by MCA analysis are shown in Fig. 4. The loading angles ψ were 18°, 30°, 45°, and 60°.

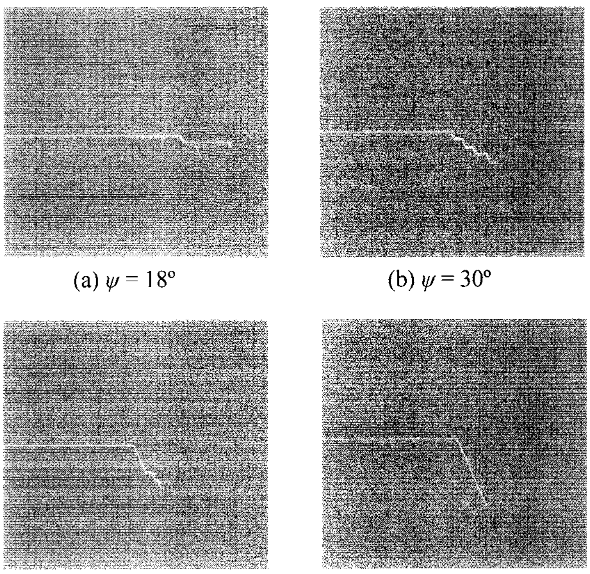

(a) $\psi = 18°$ (b) $\psi = 30°$

(c) $\psi - 45°$ (d) $\psi = 60°$

Fig. 4 Crack growth paths under different loading angles

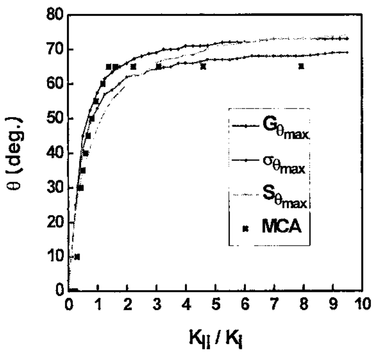

(a)

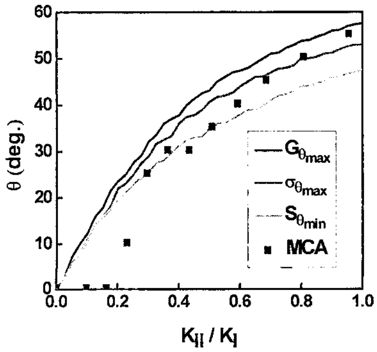

(b)

Fig. 5 Angle of crack propagation and locus of fracture diagram under mixed-mode loading

Figure 5 depicts the angle of crack propagation under mixed-mode loading using various types of criteria combined with the results of the MCA analysis. The criteria used as reference values almost coincided with each other, with the exception of load conditions near the pure shear mode. In this case, the maximum circumferential tensile stress theory yielded slightly lower values, and the results of the MCA analysis were in close agreement with all of them. However, when the loading angle was in the range $0° \le \psi \le 18°$, the crack did not bend from the interface. Therefore, the crack growth path represented the pure tension mode (Fig. 4(a)). For pure mode II ($K_I = 0$), the MCA analysis gave $\psi = 64°$. The results obtained from the maximum circumferential tensile stress theory coincided best with those of the MCA analysis.

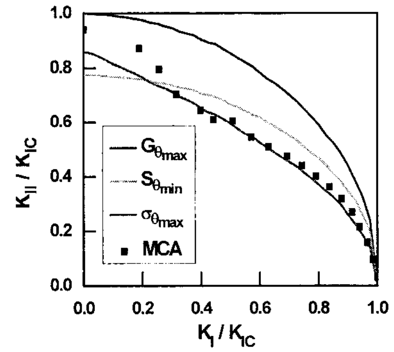

Fig. 6 Locus of fracture diagram under mixed-mode loading

The locus of fracture diagram under mixed-mode loading is shown in Fig. 6. Here, once again, the MCA results agreed with the results obtained from the maximum circumferential tensile stress theory, aside from a few differences in the near pure shear mode.

Figure 7 depicts resistance curves plotted during crack growth. In the pure tension mode (Fig. 7(a)), the MCA simulation yielded a relatively small slope for an ideally brittle material, which was expected to exhibit a flat R curve. Under mixed-mode loading with a loading angle of 30° (Fig. 7(b)), mode II effects were in evidence, and an ascending R curve was the result. Finally, the steepest slope occurred under a loading angle of 60°, where the effect of the shear mode was significant (Fig. 7(c)).

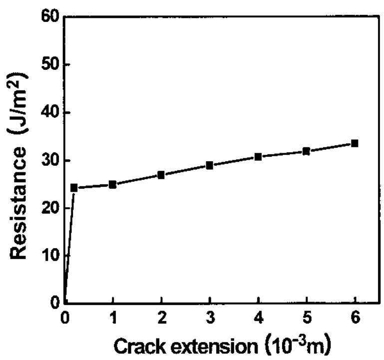

(a) Crack extension behavior under the pure tension mode

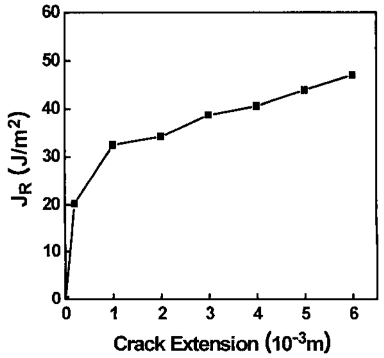

(b) Crack extension behavior under 30° loading

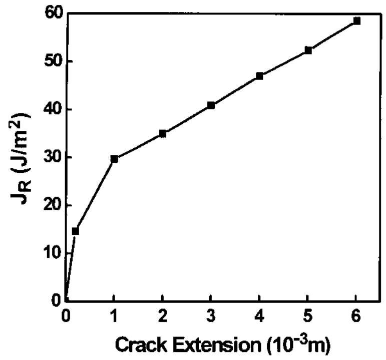

(c) Crack extension behavior under 60° loading

Fig. 7 Crack extension behavior

6. Conclusions

In this paper, the bifurcation and propagation of a mixed-mode crack in soda-lime silica glass were investigated via the movable cellular automata method. A special fracture criterion was introduced, and could be used to evaluate the beginning of crack propagation as well as crack bifurcation. The crack growth path and the bifurcation angle were found. The MCA results for the angle of crack propagation were compared with results obtained by applying the maximum circumferential tensile stress, maximum energy release rate, and minimum strain energy density criteria. The results obtained using the maximum circumferential tensile stress criterion were in closest agreement with the results of the MCA analysis. The bifurcation angle for pure mode *II* was found to be 64°. For the loading range $0° \leq \psi \leq 18°$, the crack remained in the interface, whereas for $\psi \geq 18°$, the crack was bent from the interface. Finally, crack resistance curves (under different loading angles) were plotted, and the slope was observed to increase with the effect of shear mode.

The MCA approach could be used as an alternative method for simulating crack propagation.

ACKNOWLEDGEMENT

This research was supported by the Yeungnam University research grants in 2007.

REFERENCES

1. Neumann, J., "Theory of Self-Reproducing Automata," University of Illinois Press, pp. 6-8, 1966.
2. Toffoli, T. and Margolus, N., "Cellular Automata Machines," The MIT Press, pp. 6-9, 1987.
3. Sipper, M., "Evolution of Parallel Cellular Machines: The Cellular Programming Approach," Heidelberg: Springer-Verlag, pp. 73-78, 1997.
4. Burks, A. (Ed.), "Essays on Cellular Automata," University of Illinois Press, pp. 50-53, 1970.
5. Smith, A., "Cellular Automata Theory," Technical Report 2, Stanford University, pp. 15-19, 1969.
6. Popov, V. L. and Psakhie, S. G., "Theoretical Principles of Modeling Elastoplastic Media by Movable Cellular Automata Method - I. Homogeneous Media," Phys. Mesomech., Vol. 4, No. 1, pp. 15-25, 2001.
7. Psakhie, S. G., Horie, Y., Ostermeyer, G. P., Korostelev, S. Y., Smolin, A. Y., Shilko, E. V., Dmitriev, A. I., Blatnik, S., Spiegel, M. and Zavsek, S., "Movable Cellular Automata Method for Simulating Materials with Mesostructure," Theoretical and Applied Fracture Mechanics, Vol. 37, No. 1-3, pp. 311-334, 2001.
8. Lee, S. W., Han, S. W. and Lee, H. S., "Reliability Evaluation of an Oil Cooler for a High-Precision Machining Center," International Journal of Precision Engineering and Manufacturing, Vol. 8, No. 3, pp. 50-53, 2007.
9. Kim, S. K., "Object-oriented Development of Computer Code for Inverse Heat Conduction Problem," International Journal of Precision Engineering and Manufacturing, Vol. 8, No. 1, pp. 59-65, 2007.
10. Kwak, D. S., Kim, S. H. and Oh, T. Y., "Effect of a Single Applied Overload on Fatigue Crack Growth Behavior in Laser-welded Sheet Metal," International Journal of Precision Engineering and Manufacturing, Vol. 7, No. 3, pp. 30-34, 2006.
11. Chun, D. M., Kim, M. H., Lee, J. C. and Ahn, S. H., "A Nano-particle Deposition System for Ceramic and Metal Coating at Room Temperature and Low Vacuum Conditions," International Journal of Precision Engineering and Manufacturing, Vol. 9, No. 1, pp. 51-53, 2008.
12. Son, I. S., Cho, J. R. and Yoon, H. I., "Effects of a Moving Mass on the Dynamic Behavior of Cantilever Beams with Double Cracks," International Journal of Precision Engineering and Manufacturing, Vol. 9, No. 3, pp. 33-39, 2008.
13. Beoek, D., "Elementary Engineering Fracture Mechanics," Sijthoff and Noordhoff, pp. 86-89, 1978.
14. Erdogan, F. and Sih, G. C., "On the Crack Extension in Plates Under Plane Loading and Transverse Shear," J. Basic Engineering, Vol. 85, No. 1, pp. 519-527, 1963.
15. Hussain, M., Pu, S. and Underwood, J., "Strain Energy Release Rate for a Crack Under Combined Mode I and Mode II," ASTM STP 560, Vol. 1, No. 2, pp. 2-28, 1974.
16. Sih, G. C., "Strain Energy Factors Applied to Mixed Mode Crack Problems," Int. J. Fracture, Vol. 10, No. 3, pp. 305-314, 1974.